# *Influence of Grain Structure and Doping on the Deformation and Fracture of Polycrystalline Silicon for MEMS/NEMS*

Ioannis Chasiotis
*Aerospace Engineering*
*University of Illinois at Urbana-Champaign*

*AFOSR Grant # FA9550-09-1-0535*
*Program Manager: Dr. B.L. Lee*

# Report Documentation Page

*Form Approved*
*OMB No. 0704-0188*



| | | |
|---|---|---|
| 1. REPORT DATE<br>**AUG 2012** | 2. REPORT TYPE | 3. DATES COVERED<br>**00-00-2012 to 00-00-2012** |
| 4. TITLE AND SUBTITLE<br>**Influence of Grain Structure and Doping on the Deformation and Fracture of Polycrystalline Silicon for MEMS/NEMS** | | 5a. CONTRACT NUMBER<br>5b. GRANT NUMBER<br>5c. PROGRAM ELEMENT NUMBER |
| 6. AUTHOR(S) | | 5d. PROJECT NUMBER<br>5e. TASK NUMBER<br>5f. WORK UNIT NUMBER |
| 7. PERFORMING ORGANIZATION NAME(S) AND ADDRESS(ES)<br>**University of Illinois at Urbana-Champaign,Aerospace Engineering,Urbana,IL,61801** | | 8. PERFORMING ORGANIZATION REPORT NUMBER |
| 9. SPONSORING/MONITORING AGENCY NAME(S) AND ADDRESS(ES) | | 10. SPONSOR/MONITOR’S ACRONYM(S)<br>11. SPONSOR/MONITOR’S REPORT NUMBER(S) |

12. DISTRIBUTION/AVAILABILITY STATEMENT
**Approved for public release; distribution unlimited**

13. SUPPLEMENTARY NOTES
**Presented at the 2nd Multifunctional Materials for Defense Workshop in conjunction with the 2012 Annual Grantees’/Contractors’ Meeting for AFOSR Program on Mechanics of Multifunctional Materials & Microsystems Held 30 July - 3 August 2012 in Arlington, VA. Sponsored by AFRL, AFOSR, ARO, NRL, ONR, and ARL. U.S. Government or Federal Rights License**

14. ABSTRACT

15. SUBJECT TERMS

| 16. SECURITY CLASSIFICATION OF: | | | 17. LIMITATION OF ABSTRACT | 18. NUMBER OF PAGES | 19a. NAME OF RESPONSIBLE PERSON |
|---|---|---|---|---|---|
| a. REPORT<br>**unclassified** | b. ABSTRACT<br>**unclassified** | c. THIS PAGE<br>**unclassified** | **Same as Report (SAR)** | **29** | |

# *Goals, Accomplishments, On-going Research*

## Research Objectives

- Investigate the dependence of mode I fracture toughness of polysilicon thin films on grain size and doping
- Quantify mechanical strength size effects for laminated and columnar grain polysilicon subjected to different doping conditions.

## Accomplishments

- Measured the effective mode I critical stress intensity factor for laminated and columnar grain polysilicon films as a function of dopant concentration
- Quantified the effect of specimen size on fracture strength of polysilicon films via a Weibull analysis to identify the location of failure initiation
- Employed fusion bonded (Si-Si) chevron notch specimens to study the effect of doping and crystallographic orientation on $K_{IC}$ of Si grain boundaries
- Characterized the electromechanical behavior of PZT thin films for MEMS.

## On-going Research

- Measure the $K_{IC}$ of polysilicon grain boundaries as a function of dopant concentration with fracture experiments on Si-Si wafer bonded specimens with Chevron notches
- Removal of sidewall defects in columnar grain polysilicon to determine the improvement in mechanical strength.

# Fabrication of Columnar and Laminated Polysilicon

Columnar Polysilicon

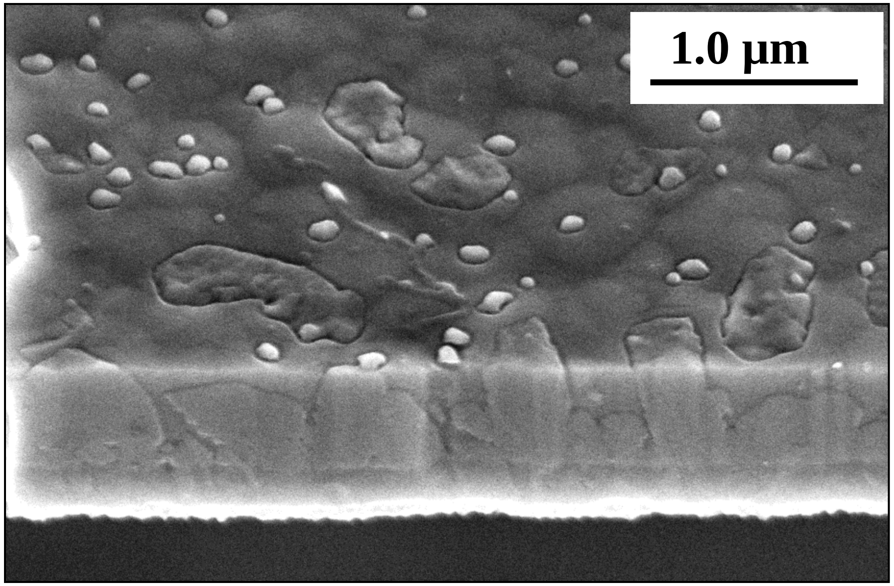


Laminated Polysilicon

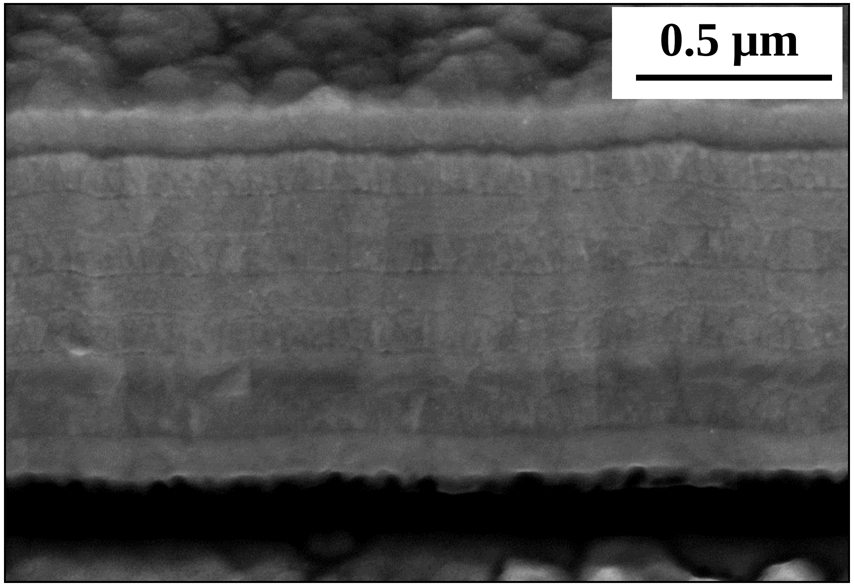


- Polysilicon films were fabricated using a modified Sandia's SUMMiT V™ microfabrication process.
- 1 µm thick polysilicon films were micromachined into dog-bone shaped specimens with gage length and width of 1,000 µm and 100 µm respectively.
- Both polysilicon types of film were doped with various concentrations of P diffused from a sacrificial phosphosilicate glass (PSG) layer during annealing.

# Fabrication of Columnar and Laminated Polysilicon

## Columnar Polysilicon

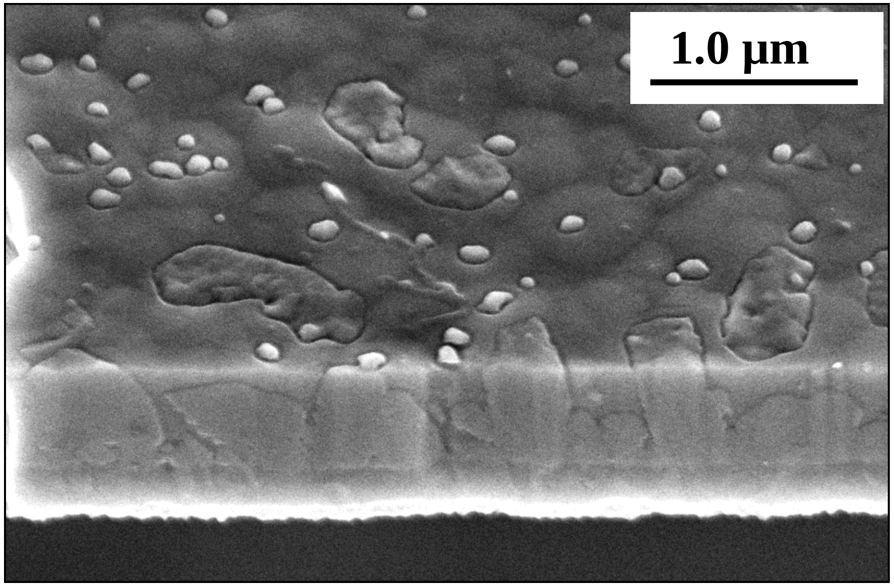


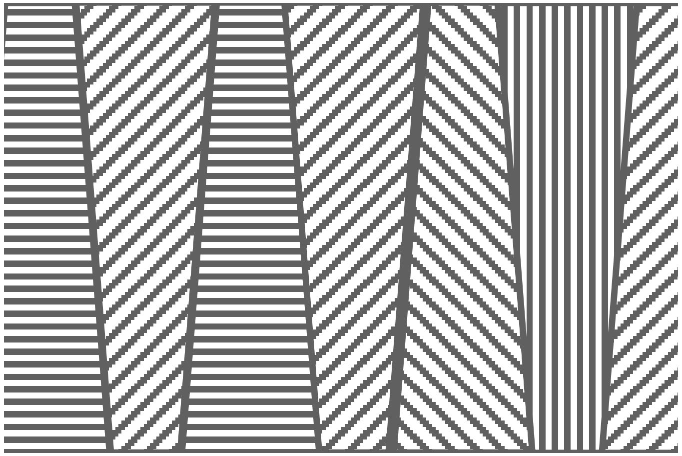

## Laminated Polysilicon

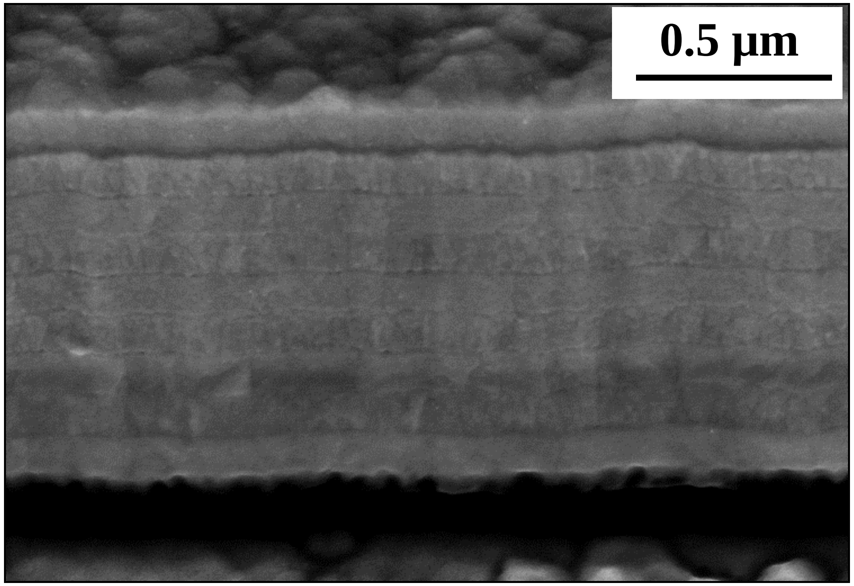


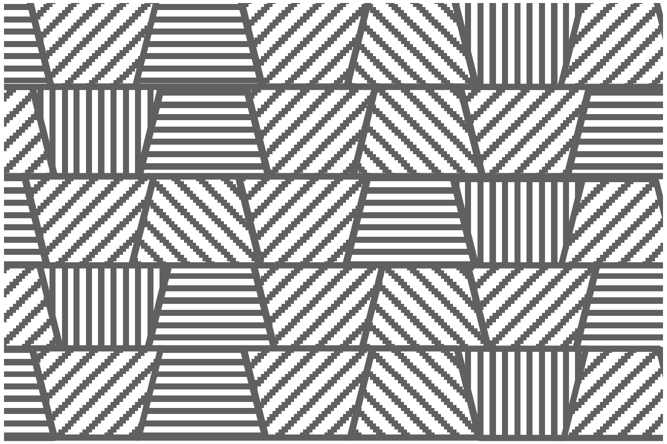

# Polysilicon Films with Different Grain Size and Doping

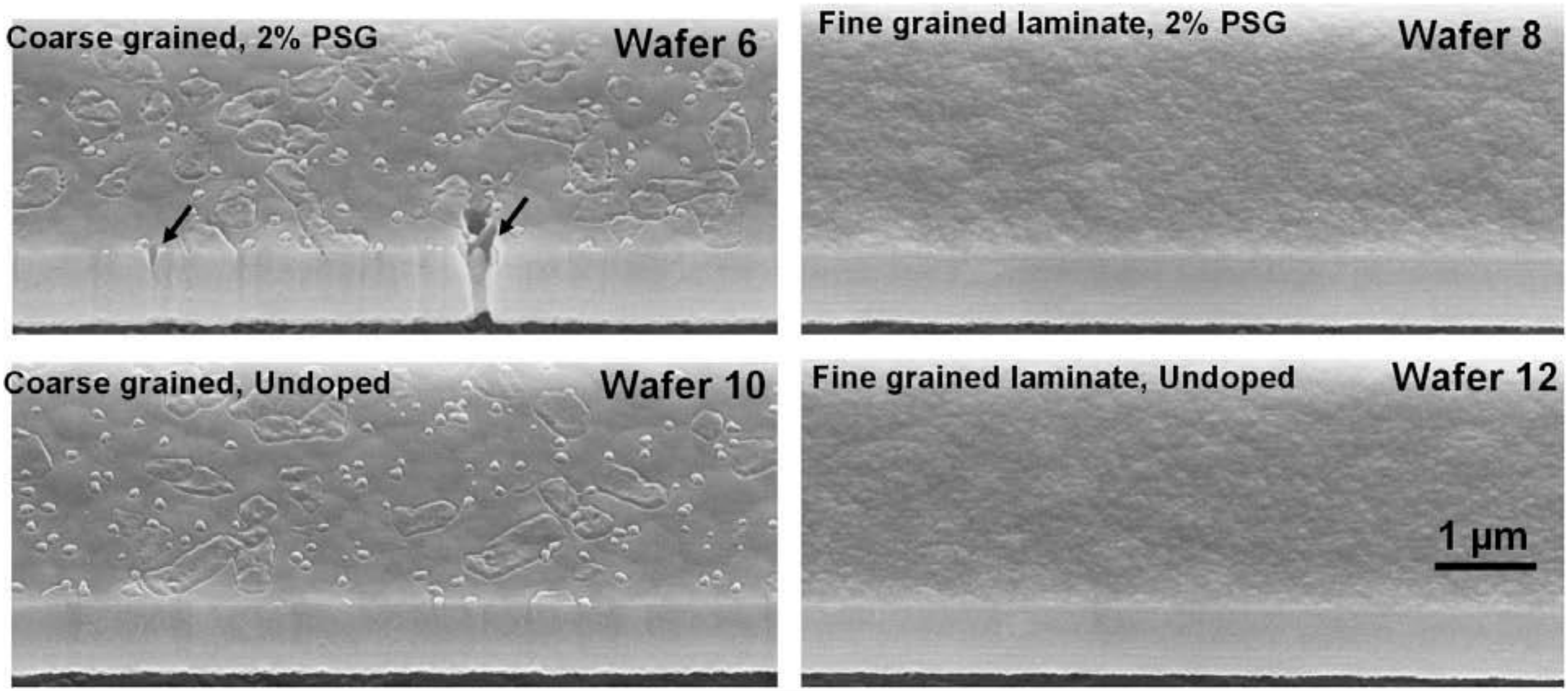


- Polysilicon film specimens (1 μm thick) were fabricated in a special run at the Sandia National Laboratories
- Two types of polysilicon films : Large grain and small grain (laminated)
- The laminar structure controlled the grain size.

B.L. Boyce, et al., “Stronger silicon for microsystems”, Acta Materialia 58, pp. 439-448, (2010)

# *Fracture Specimens for Microscale Experiments*

- Mathematically sharp cracks were generated by indentation performed on the substrate near a specimen free edge
- Edge cracks with an average length of 25 µm were introduced to 1 µm thin polysilicon specimens
- Cracks were imaged by SEM and AFM to obtain their geometry and the grain structure at the crack tip.

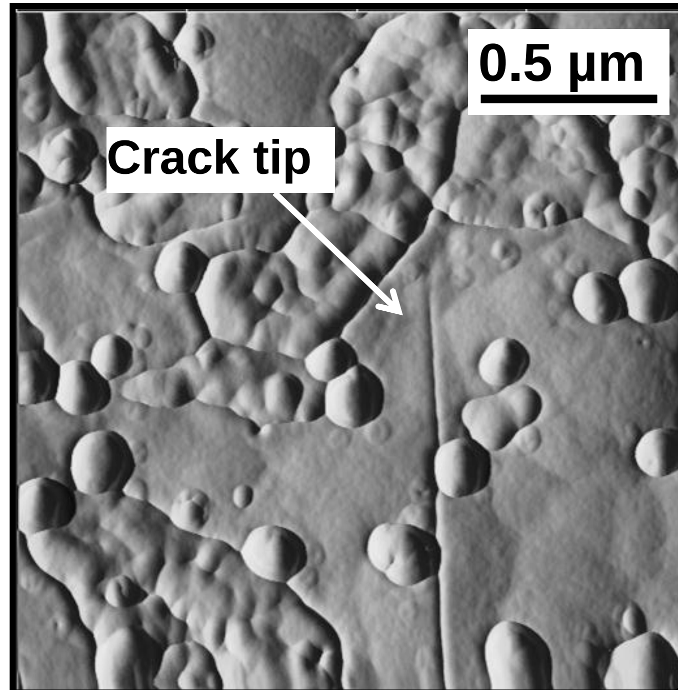


**Indentation to create edge crack in polycrystalline silicon thin film specimens**

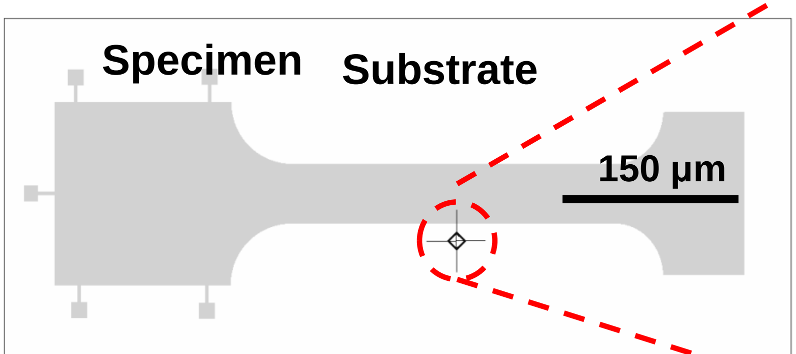


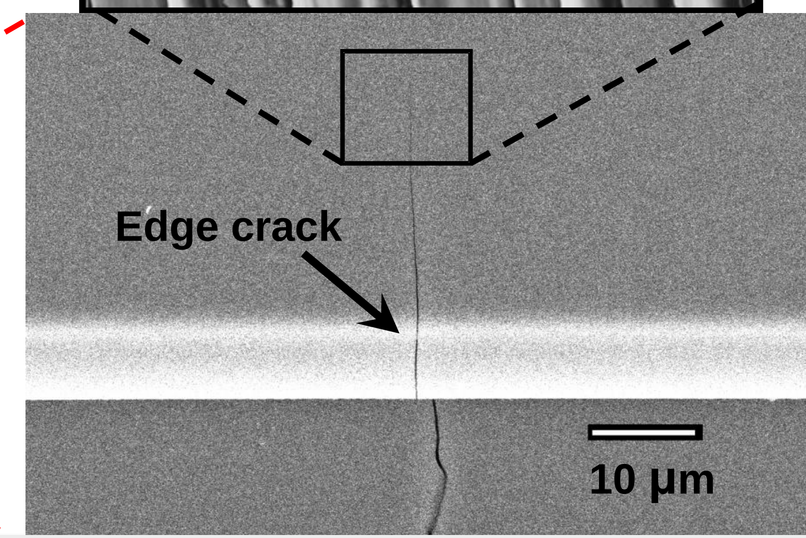



I. Chasiotis, S.W. Cho, K. Jonnalagadda, "Fracture Toughness and Crack Growth in Polycrystalline Silicon", Journal of Applied Mechanics 73 (5) , pp. 714-722, (2006).

# Crack Tip in Polysilicon Films with Different Grain Structures

**Columnar polySi, 2% PSG**

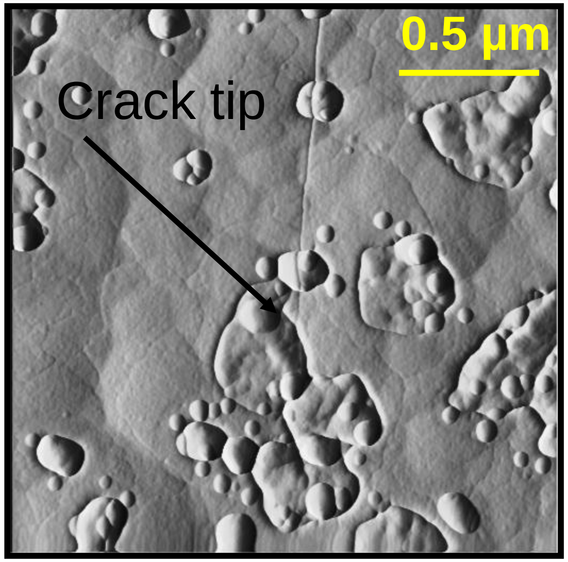


**Laminated polySi, 2% PSG**

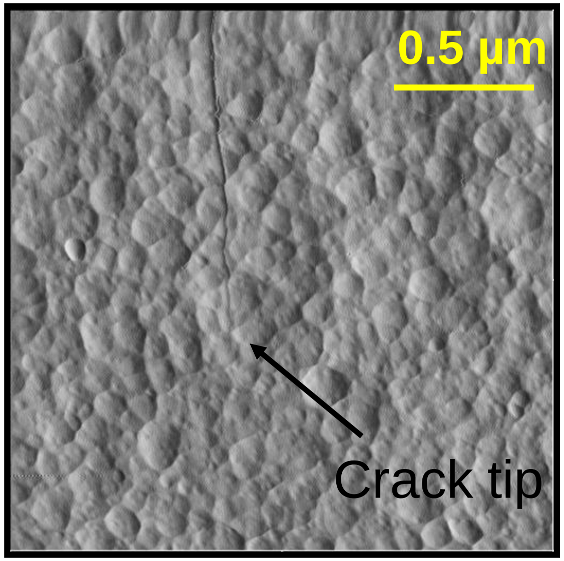


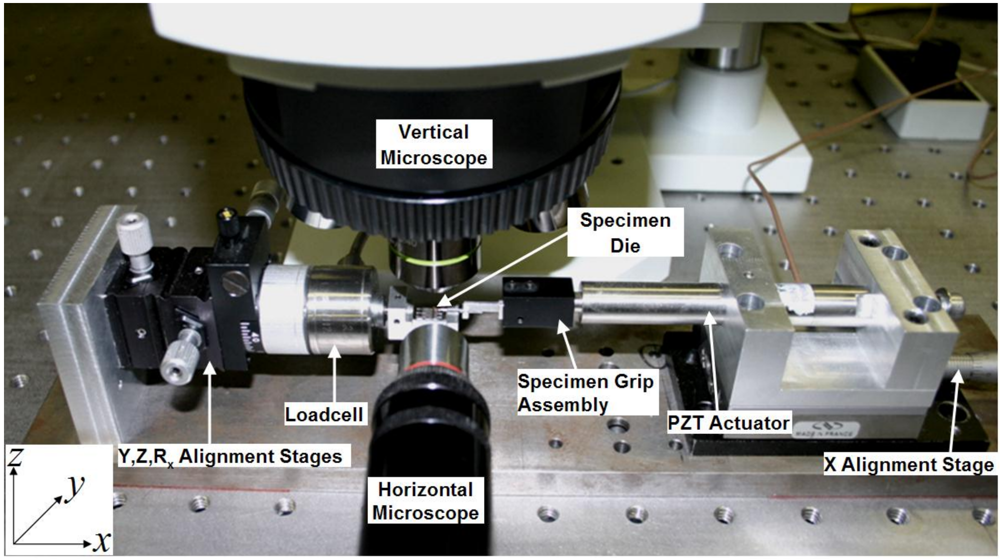


- The precise location of the crack tip, its geometry and adjacent material were determined using AFM images obtained at different magnifications
- Experimental setup used to test pre-cracked polysilicon thin films under mode I loading.

K. Jonnalagadda, I. Chasiotis, S. Yagnamurthy J. Lambros, R. Polcawich, J. Pulskamp, and M. Dubey, "Experimental Investigation of Strain Rate Dependence in Nanocrystalline Pt Films," Experimental Mechanics 50 (1), pp. 25-35, (2010).

# *Effect of Grain Structure and Doping on $K_{IC,eff}$*

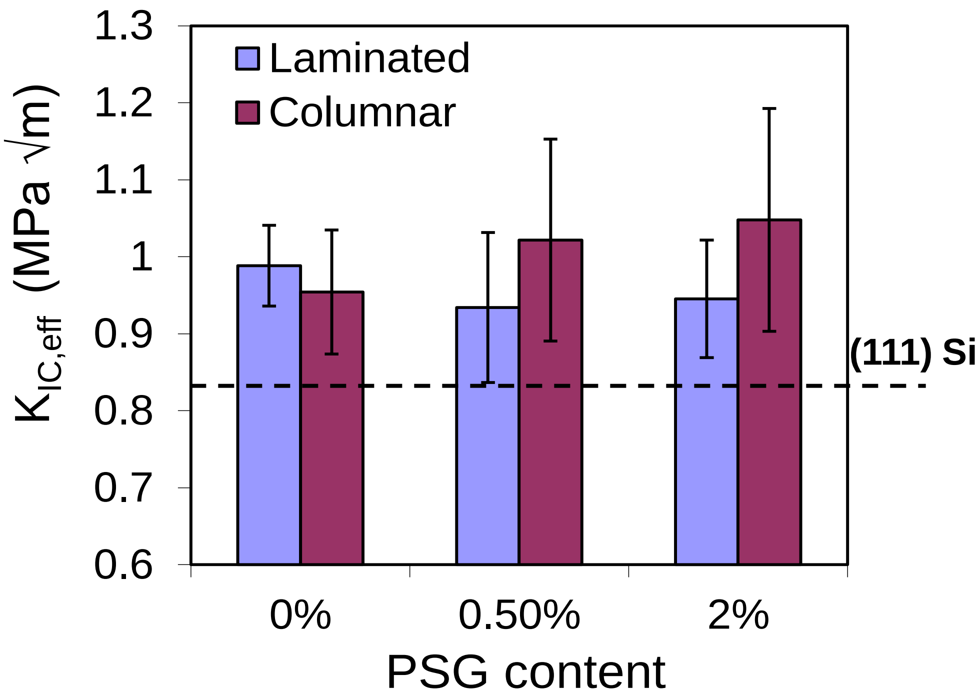


| | $K_{IC,eff}$ (MPa√m) Laminated | Columnar |
|---|---|---|
| **Undoped** | 0.99±0.05 | 0.95±0.08 |
| **0.5% PSG** | 0.93±0.10 | 1.02±0.13 |
| **2% PSG** | 0.97±0.08 | 1.05±0.14 |

- $K_{IC,eff}$ of columnar polysilicon was higher than that of laminated polysilicon.
- Minimum $K_{IC}$ for single crystal silicon is 0.84 MPa√m
- Phosphorous atoms diffuse into substitutional sites in Si forming P-Si bonds that have higher bond energy: bond energies of Si-Si and P-Si are 326.86 kJmol$^{-1}$ and 363.6 kJmol$^{-1}$ respectively.

# *Sub-Critical Crack Growth in Columnar Polysilicon*

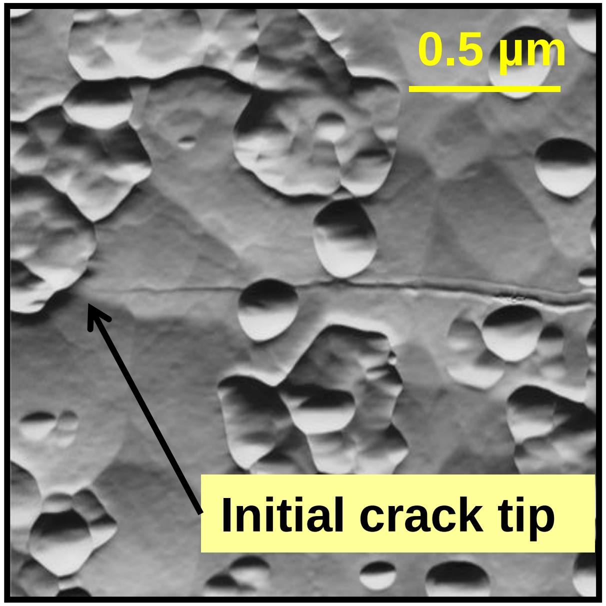


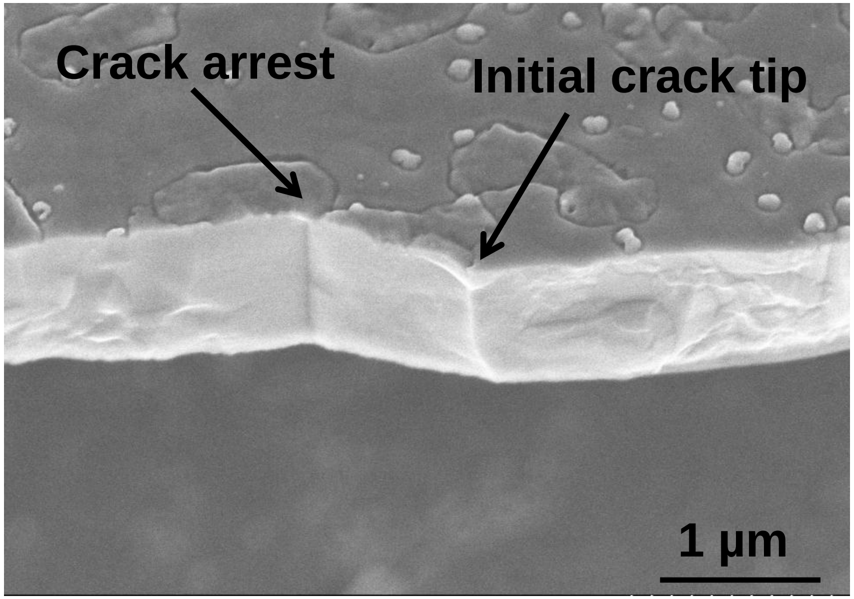


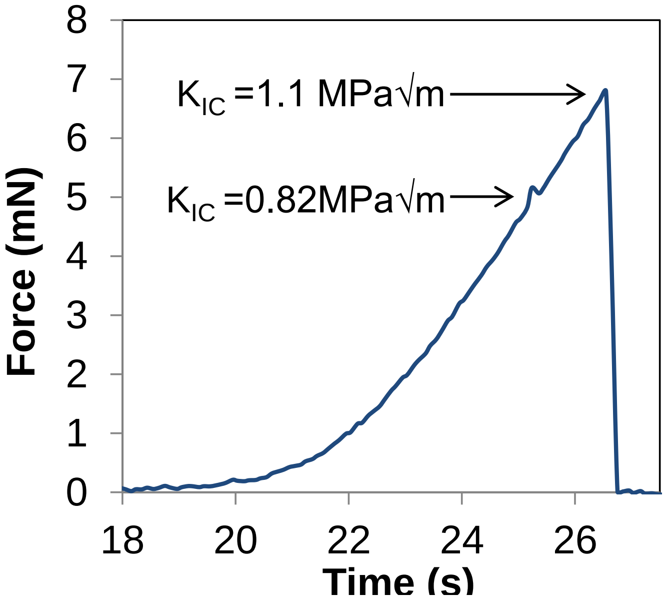


- Local crack tip deflection was observed in heavily doped (2%) large grain polysilicon
- Initial crack propagation was along the most energetically favorable plane, with the crack subsequently arrested at a grain boundary.

# *Grain Structure and Doping Effect on Fracture Strength*

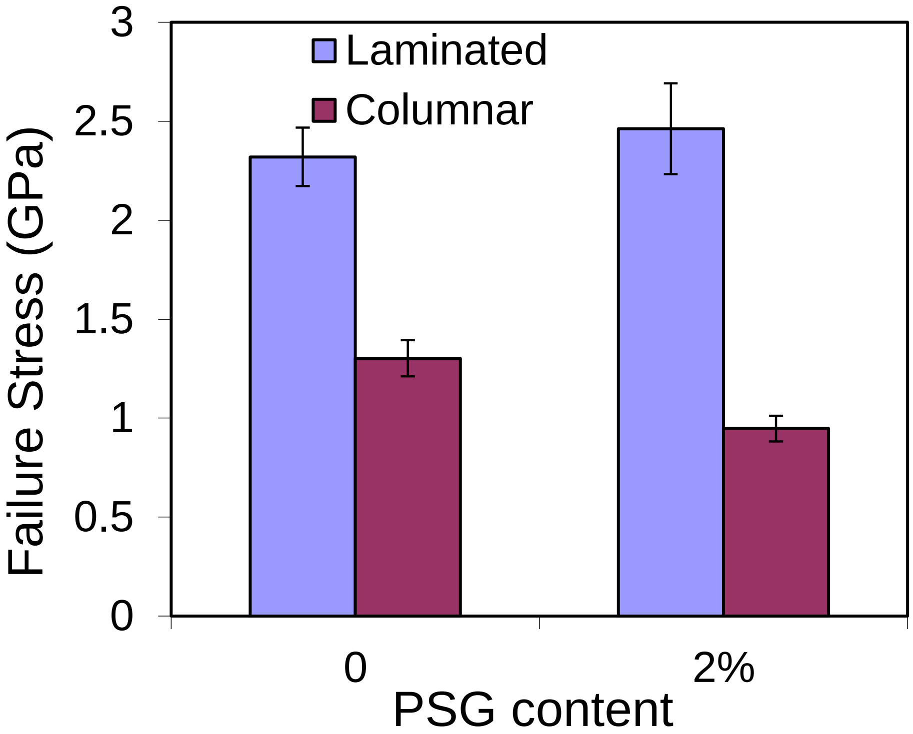


Average strength of polysilicon

| | Undoped (GPa) | 2% PSG (GPa) |
|---|---|---|
| Laminated (~125nm) | 2.32±0.15 | 2.46±0.22 |
| Columnar (~285nm) | 1.30±0.09 | 0.95±0.07 |

- The fracture strength of laminated polysilicon was 80-150% higher than columnar
- Heavily doped columnar polysilicon film exhibited ~25% lower fracture strength compared to undoped
- This implies that the increase in the upper bound of $K_{IC}$ is due to crack kinking.

# *Critical Defects on Sidewalls of Columnar Polysilicon*

Columnar polysilicon (undoped)

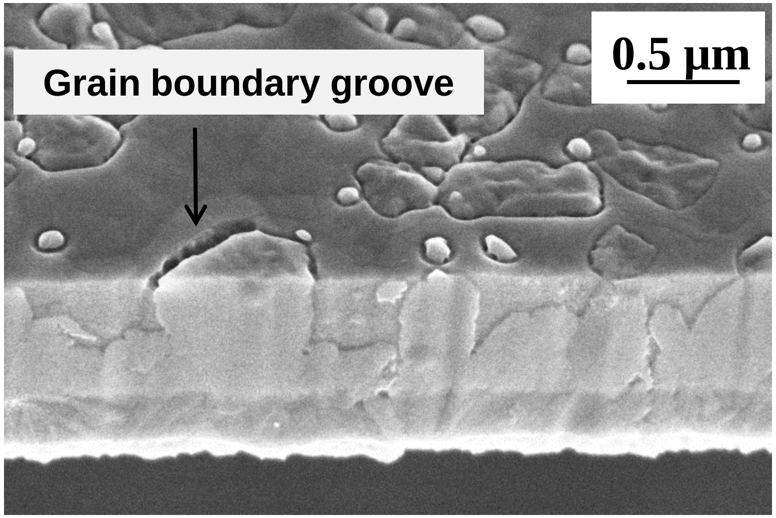


Laminated polysilicon

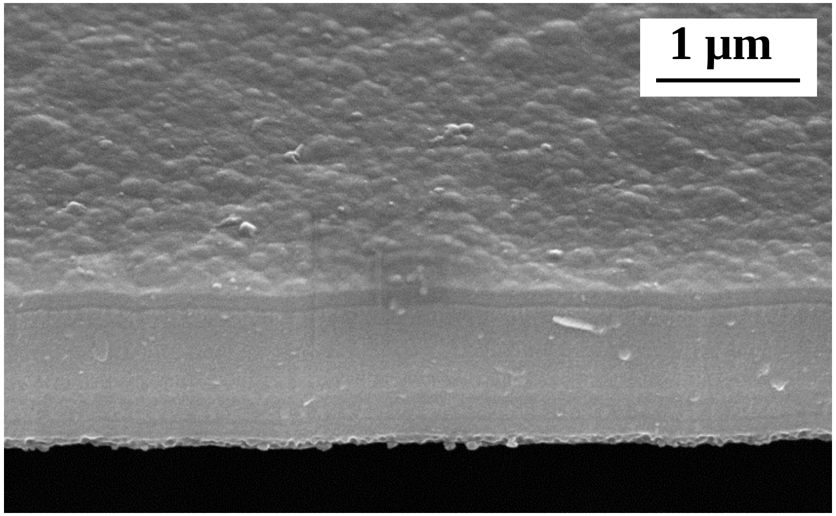


Columnar polysilicon (2% PSG)

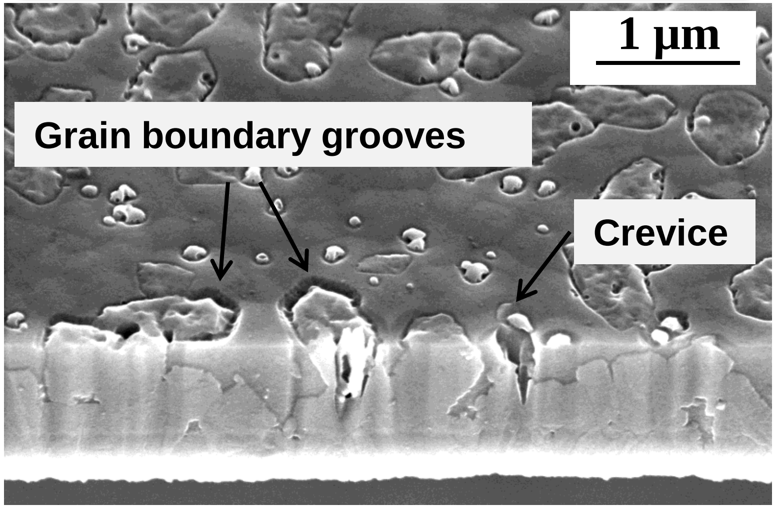


- 100-300 nm deep crevices were found on the side walls of heavily doped columnar polysilicon films.
- Doping had no impact on the surface of laminated polysilicon films.

# *Scaling of Mechanical Strength of Polysilicon*

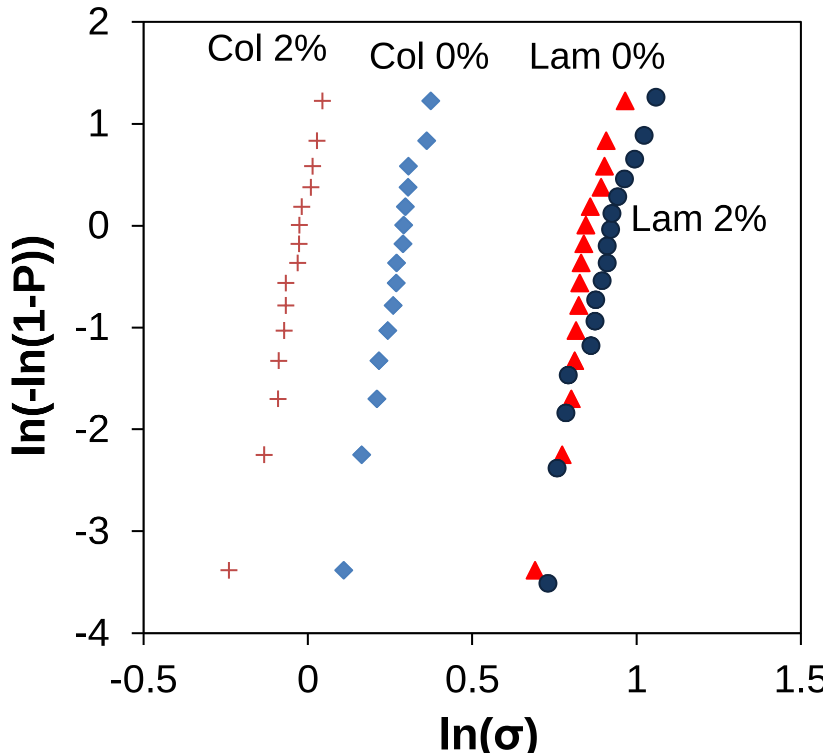


$$P = 1 - \exp\left( -\left( \frac{\sigma - \sigma_0}{\sigma_c} \right)^m \right)$$

$\sigma$ – measured strength
$\sigma_c$ – characteristic strength
$\sigma_o$ – smallest failure stress
m – Weibull modulus

Our study (shaded rows) Boyce et al (specimens ~180 times smaller) (unshaded rows)

| | 0% Columnar | 2% Columnar | 0% Laminated | 2% Laminated |
|---|---|---|---|---|
| **$\sigma_c$ (GPa)** | 1.34 | 1.01 | 2.32 | 2.51 |
| **m** | 17.63 | 16.89 | 10.314 | 9.09 |
| **$\sigma_c$ (GPa)** | 1.76 | 1.48 | 2.80 | 2.83 |
| **m** | 12.9 | 8.7 | 8.6 | 13.5 |

# *Scaling of Mechanical Strength of Polysilicon*

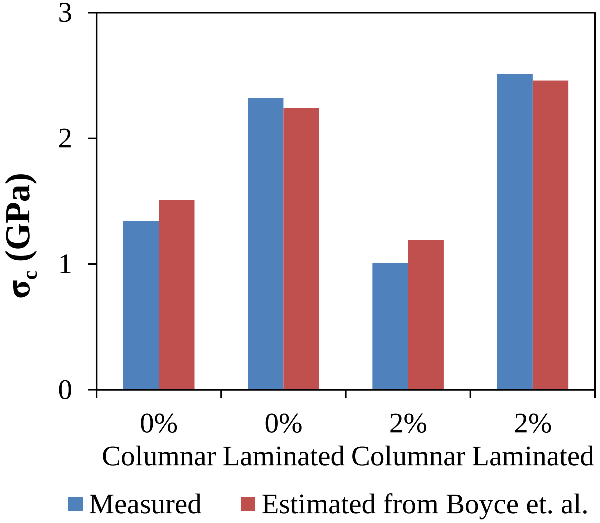


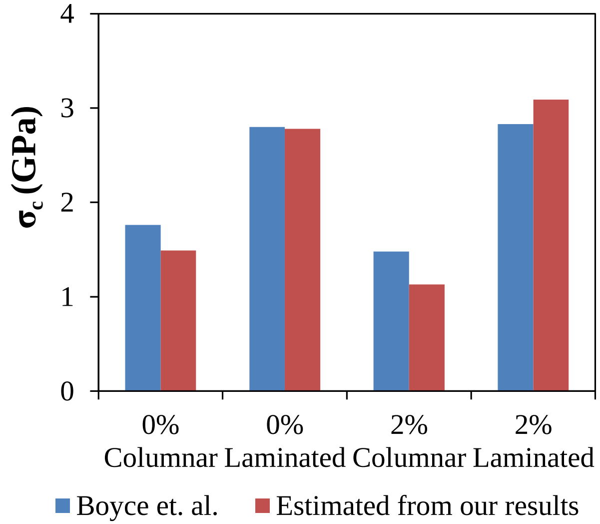


$$\sigma_{c2} = \sigma_{c1} \times \left( \frac{A_1}{A_2} \right)^{\frac{1}{m}}$$

$A_n$ is side wall area

Defects scale with side wall area

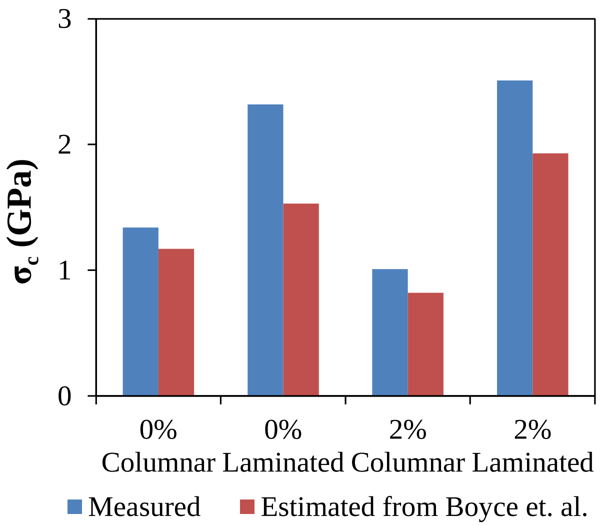


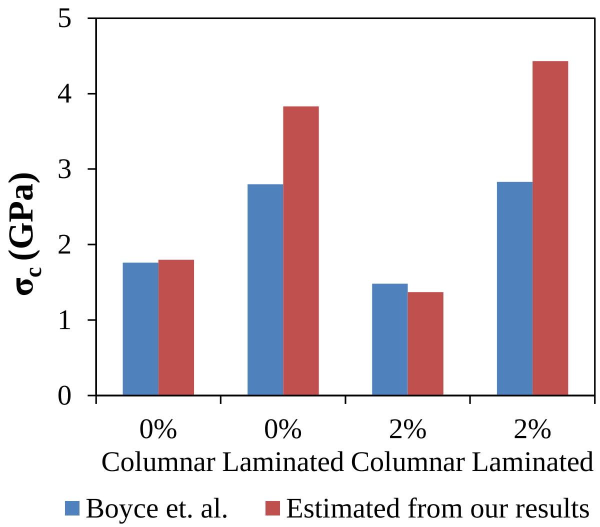


$$\sigma_{c2} = \sigma_{c1} \times \left( \frac{A_1}{A_2} \right)^{\frac{1}{m}}$$

$A_n$ is top surface area

# *Comparison with Existing Polysilicon Processes*

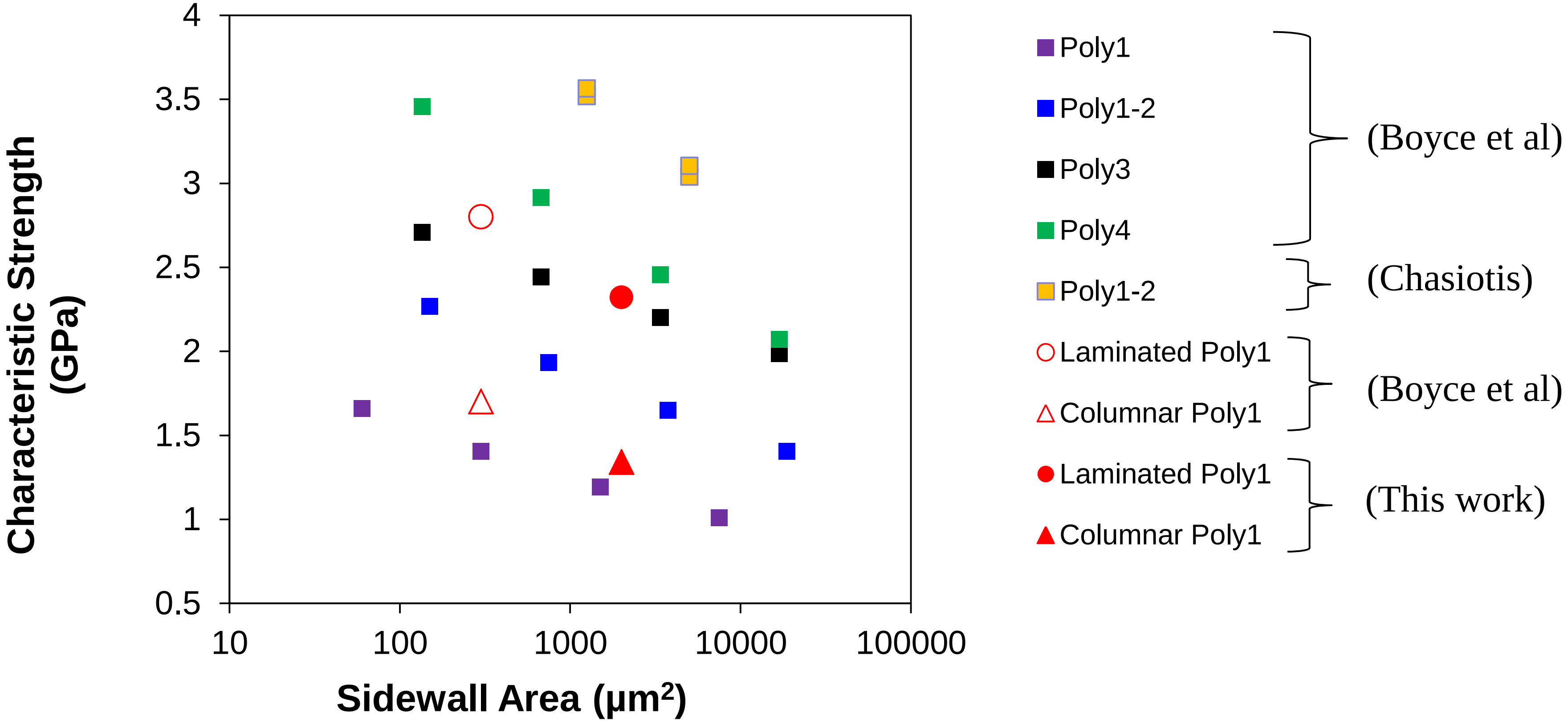


The characteristic strength of laminated poly1 improved and matched that of poly3, whereas the strength of columnar poly1 is comparable to that of regular poly1.


- I. Chasiotis, W.G. Knauss, Journal of the Mechanics and Physics of Solids 51, pp. 1551-1572, (2003).
- B. Boyce, et al, “Strength Distributions in Polycrystalline Silicon MEMS”, JMEMS, 16, pp. 179-190, 2007
- B.L. Boyce, et al., “Stronger silicon for microsystems”, Acta Materialia 58, pp. 439–448 (2010)

# *Columnar Polysilicon with Defect Free Sidewalls*

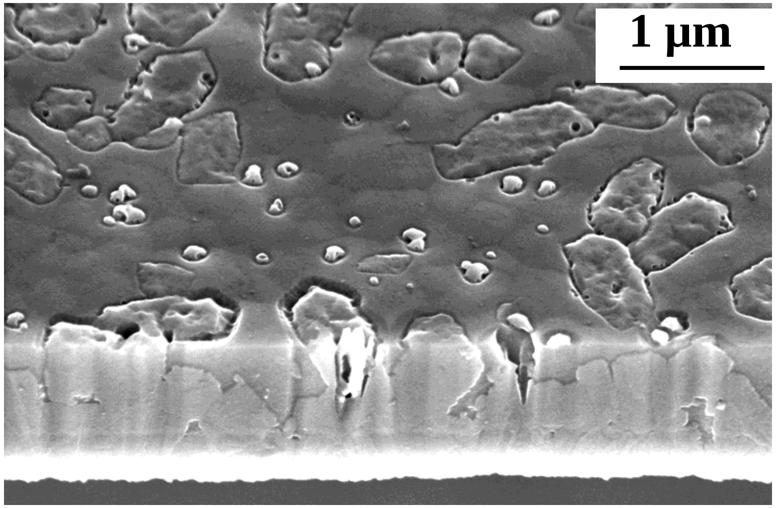


Side walls machined using FIB

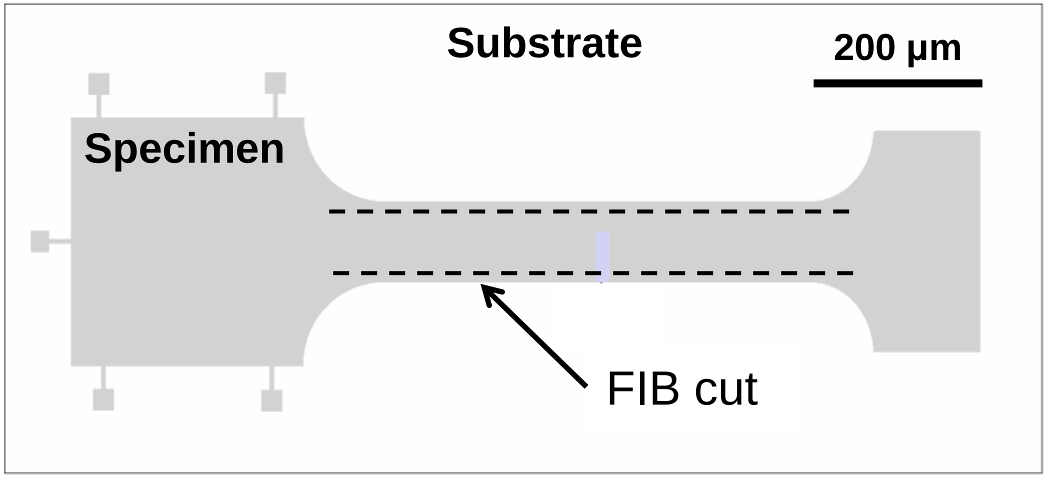


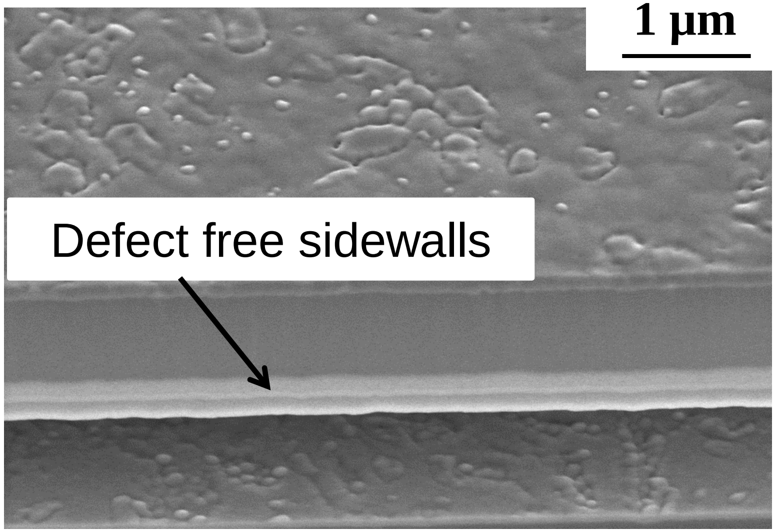


Columnar polysilicon, 2% PSG

- Sidewalls of columnar polysilicon were machined using FIB to fabricate defect free specimens
- Currently resolving challenges in gripping the specimens to test them in uniaxial tension using the narrow section.

# Ongoing Work: Cohesive Law for Silicon Grain Boundaries

Chevron notch specimens

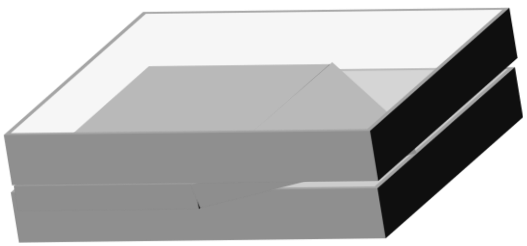

Top view

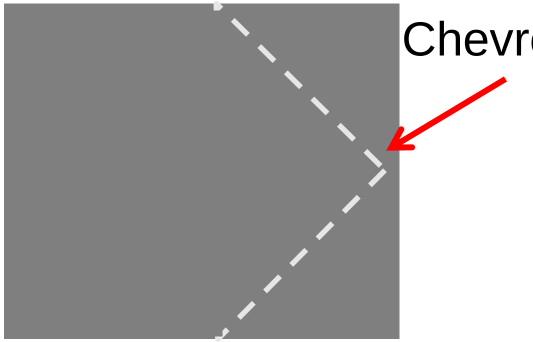


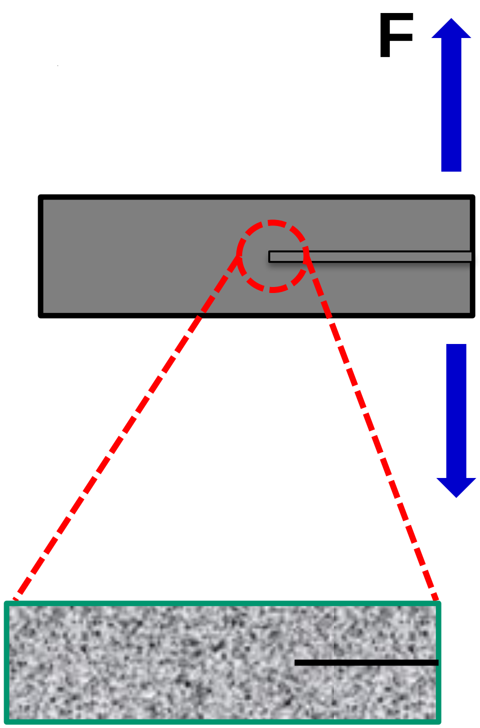


DIC of chevron tip for CTOD

Traction separation law

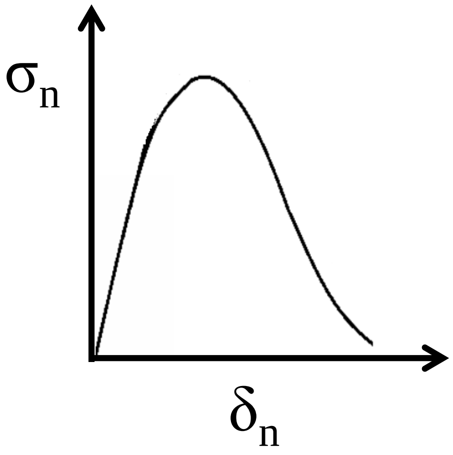


$$\sigma(\delta_n) = \frac{\partial J}{\partial \delta_n}$$

Traction separation law for the polysilicon grain boundaries obtained from J integral and CTOD measured using DIC.

# Effect of Doping on $K_{IC}$ of Si Toughness

Indentation using Vickers tip


Top View

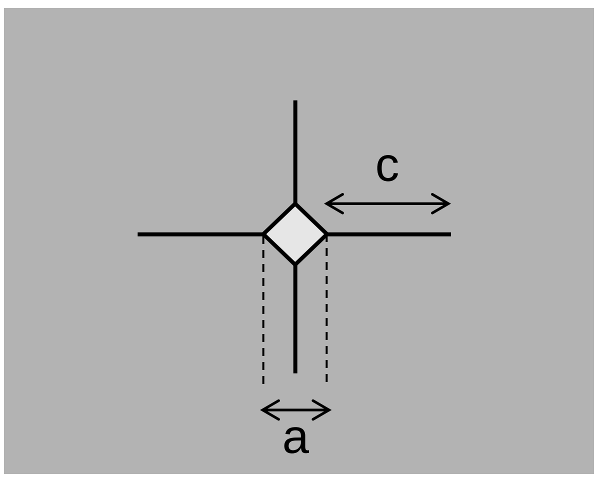


For median cracks with *c/a* >2,

$$K_{\mathrm{Ic}} = 0.129\ (c/a)^{-3/2}\ (\phi E_{[hkl]}/H)^{2/5}\ (Ha^{1/2}/\phi)$$

where $E_{[hkl]}$ is the Young's modulus along [hkl], H is the hardness of Si, φ is a plastic constraint factor (~3).

$$1/E_{[hkl]} = S_{11} - 2(S_{11} - s_{12} - 1/2S_{44})\gamma_{\alpha\beta\theta}$$

$$\gamma_{\alpha\beta\theta} = \mathrm{Cos}^2\ \alpha\ \mathrm{Cos}^2\ \beta + \mathrm{Cos}^2\ \beta\ \mathrm{Cos}^2\ \theta + \mathrm{Cos}^2\ \theta\ \mathrm{Cos}^2\ \alpha$$

$$\mathrm{Cos}\ \alpha = h/(h^2+k^2+l^2)^{\frac{1}{2}},\ \mathrm{Cos}\ \beta = k/(h^2+k^2+l^2)^{\frac{1}{2}},\ \mathrm{Cos}\ \theta = l/(h^2+k^2+l^2)^{\frac{1}{2}}$$

**F. Ebrahimi, and L. Kalwani, Mat. Sci. Eng. : A, 268 (1-2), 1999**

Indentation will be performed on silicon wafers doped with different concentrations of P

Effect of doping on $K_{IC}$ of different Si planes is being studied by driving median cracks along [001], [110] and [111] directions.

# $K_{IC}$ Measurement of Si-Si Interface Strength

Chevron notch specimens

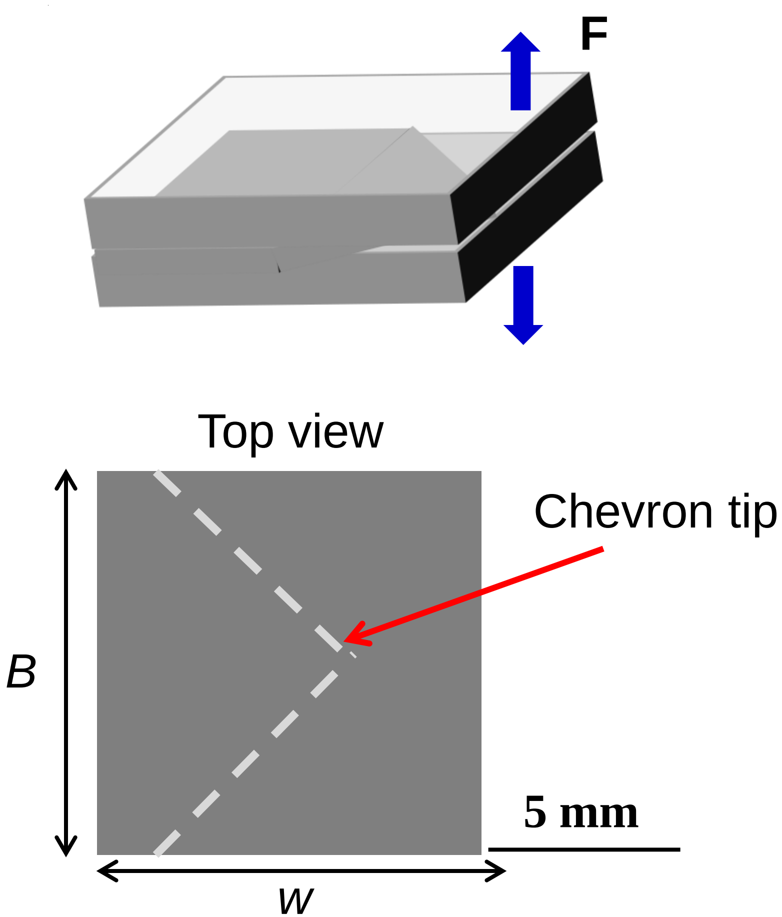


$K_I$ for a chevron notch

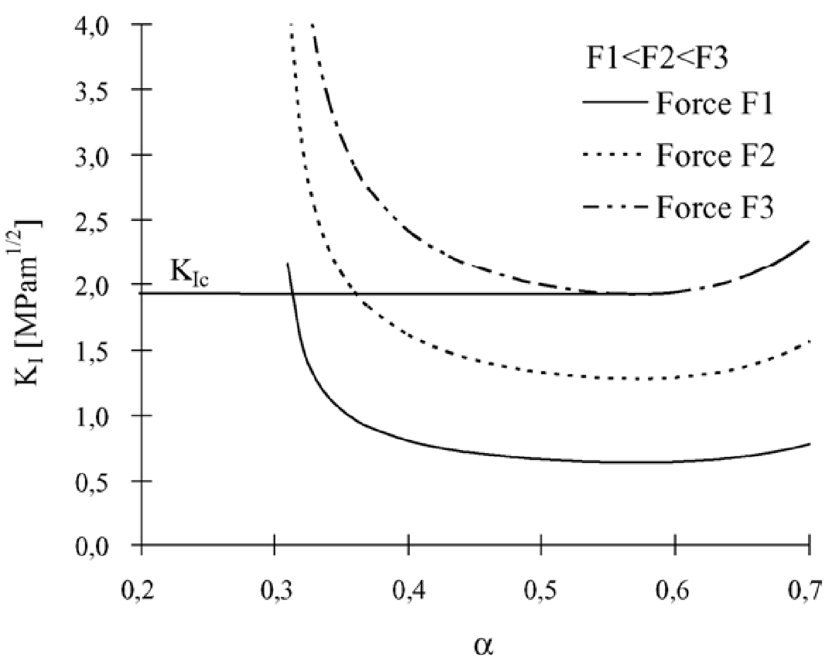


$$K_C = \frac{F_{max}}{B\sqrt{w}} Y_{min}$$

O. Vallin et al, Mater. Sci. Eng., 50, 2005

Fracture toughness of Si – Si interfaces is measured using chevron notch specimens

# Fabrication of Chevron Notch Specimens

**silicon wafer**

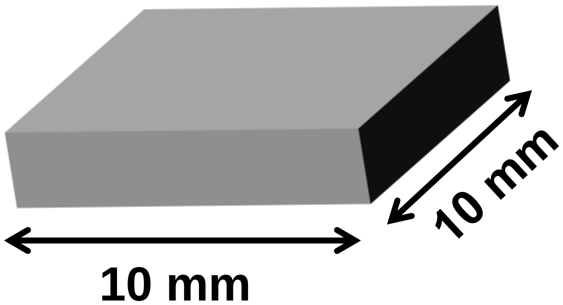


**Spin coat photoresist**

**Photolithography**

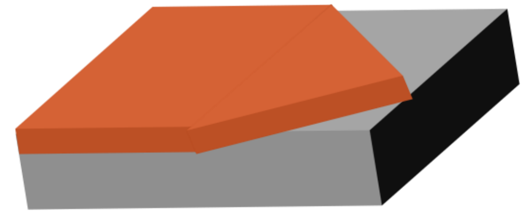

**Pattern Si wafer using Bosch's process**

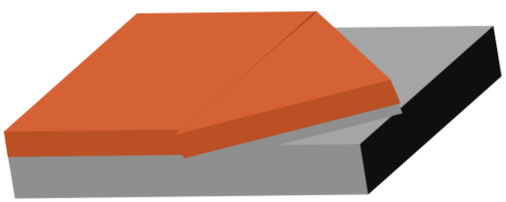

**Patterned silicon wafer**

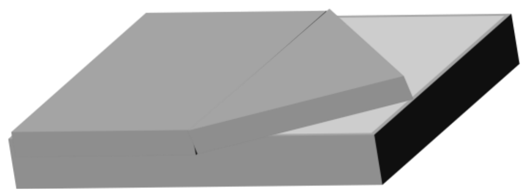

**Direct bonding of Si wafers**

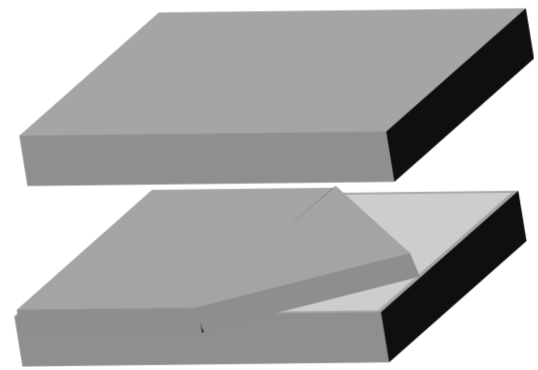

Fusion bonded silicon wafers with different concentrations of P are used to study the effect of P doping on fracture toughness of Si-Si interfaces

# *Characterization of Si-Si Bond Interface*

IR image of crack tip

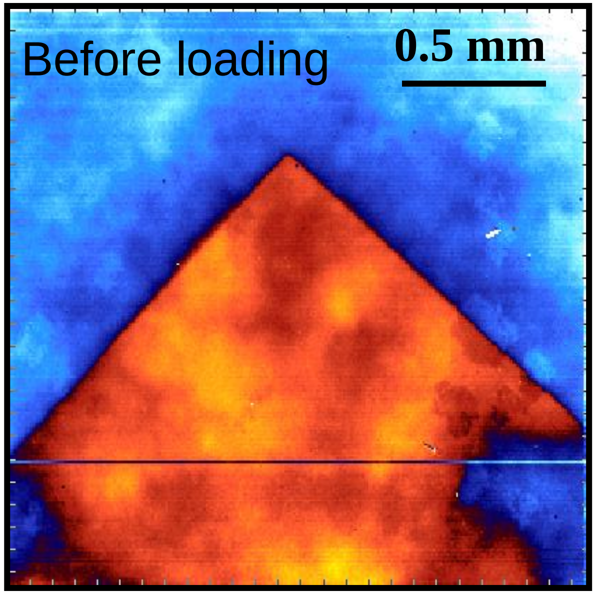


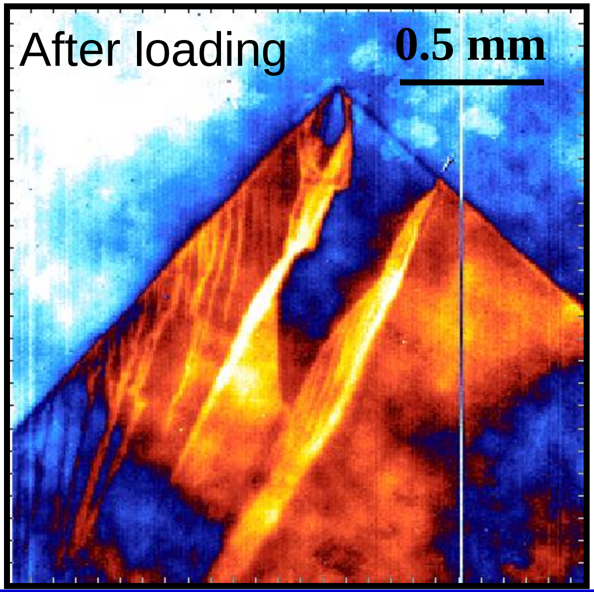


Optical image of fracture plane

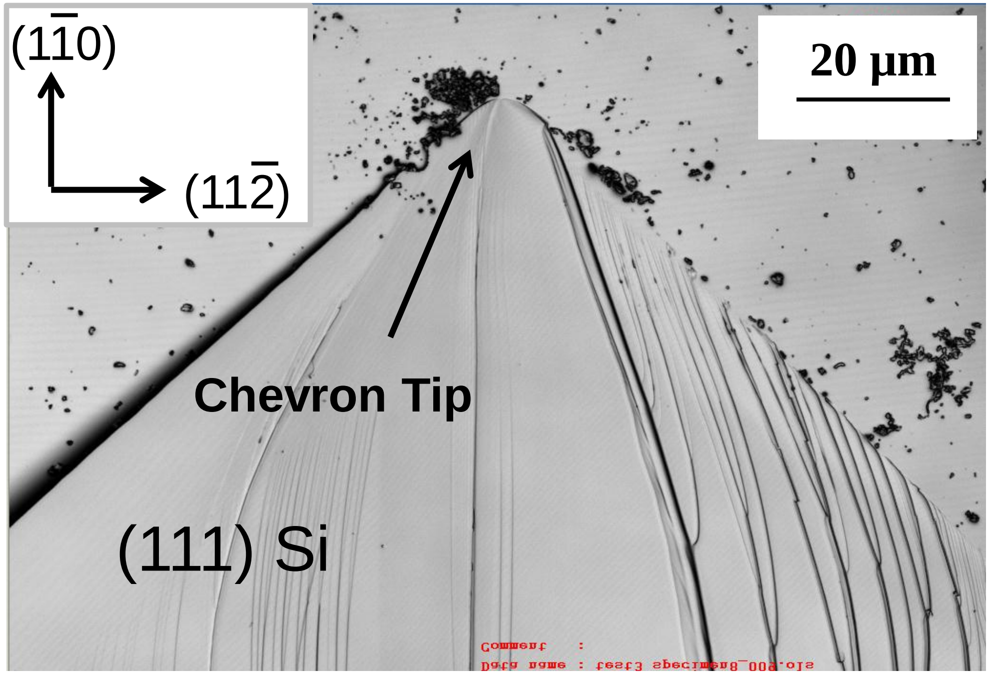


- IR images are used to characterize the quality of the interface
- Silicon cleaves easily on (111) planes and along [110] direction.

# Characterization of Si-Si Bond Interface

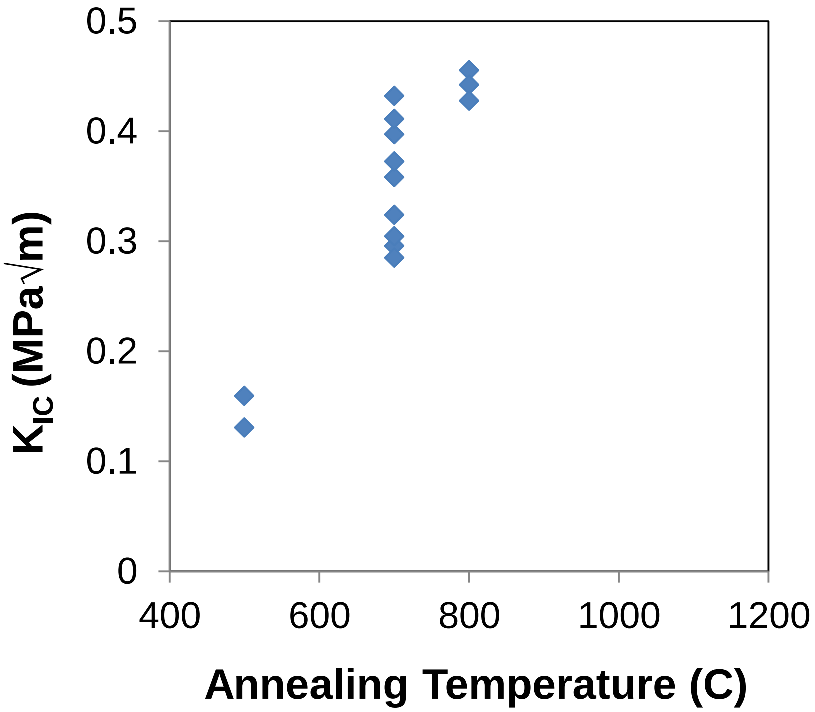


Fracture through the interface

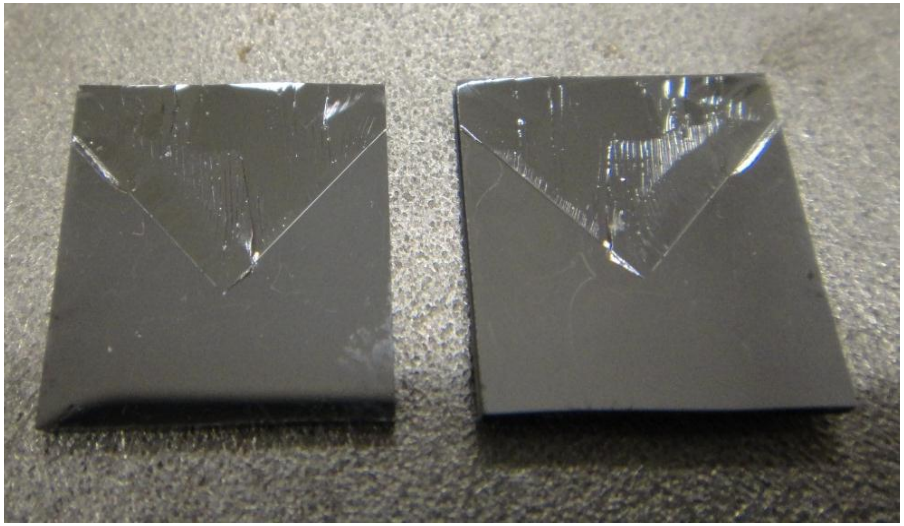

- Strength of Si-Si bond interface is dependent on annealing temperature
- Si-Si interface with different concentrations of P, and crystal orientations are being fabricated and tested to understand their effect on $K_{IC}$ of silicon.

# Mechanical & Ferroelectric Behavior of PZT Films for MEMS

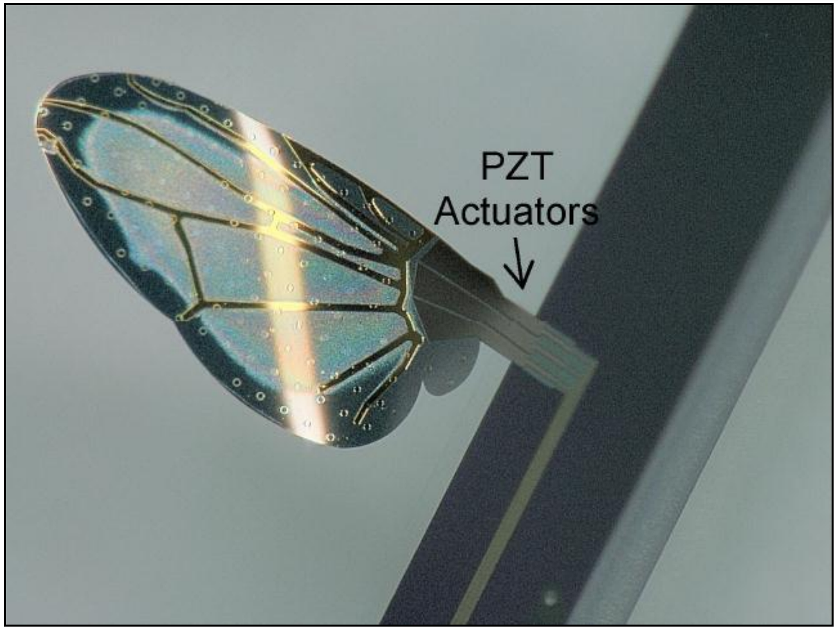


PZT thin film bimorph for MAV* wing

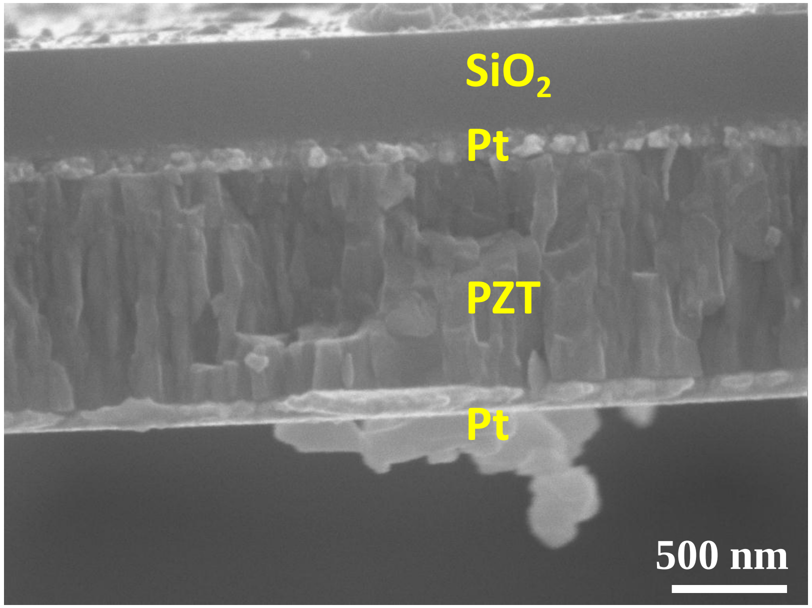


Cross section of $SiO_2$-Pt-PZT-Pt

- PZT thin films are used in MEMS devices, such as micro-sensors, actuators, and RF-MEMS
- Always fabricated in combination with other films as stacks, they undergo non-standard thermal processing
- Their mechanical and failure properties in PZT stacks are either unknown or widely scattered
- Knowledge of ferroelectric behavior is key in designing reliable devices.

J. Pulskamp et al., Proc. ASME, IDETC/CIE (2009), San Diego, DETC2009-87231

# Microscale Measurements

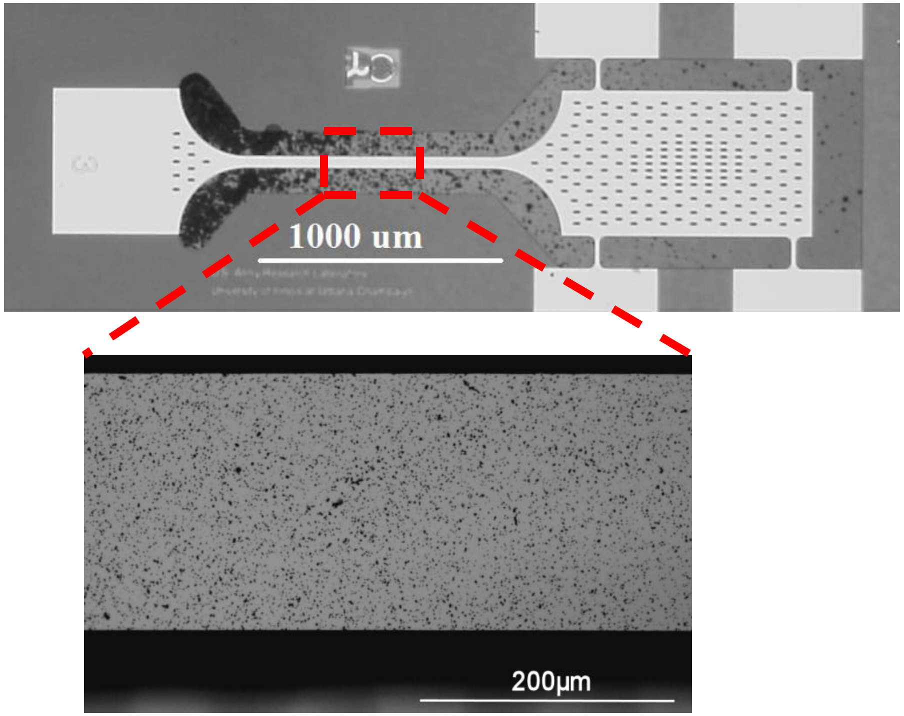


Speckle pattern for direct strain measurement

- Specimens were loaded in uniaxial tension
- Strain was calculated by DIC from the speckle pattern on the samples
- Displacement resolution ~25 nm.

Axial displacement field

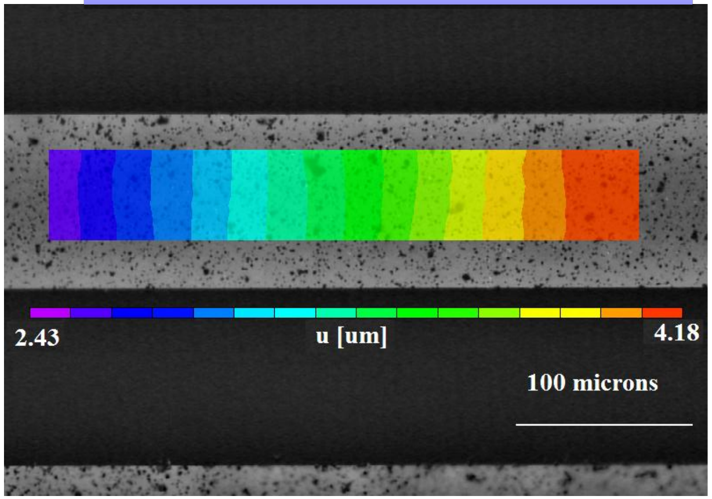


Transverse displacement field

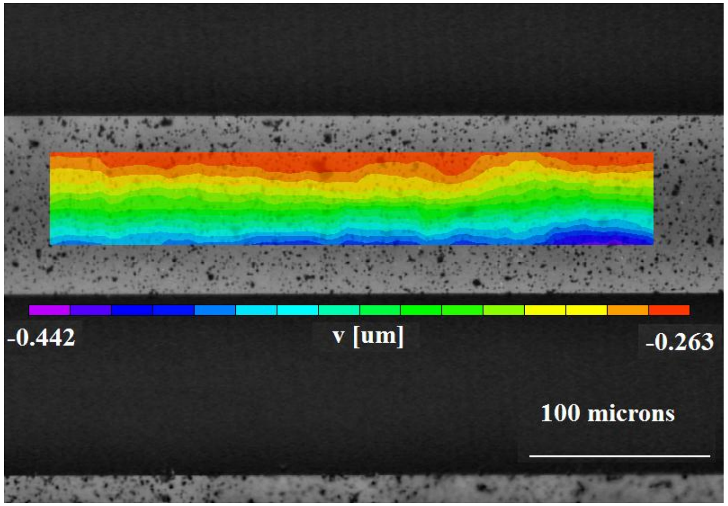


S. Yagnamurthy, I. Chasiotis, J. Lambros, R. Polcawich, J. Pulskamp, M. Dubey, “Mechanical and Ferroelectric Behavior of PZT Thin Films,” Journal of Microelectromechanical Systems 20, pp. 1250-1258, (2011).

# *Mechanical Behavior of $SiO_2$-Pt-PZT-Pt*

Open circuit condition


Short circuit condition


PZT stack (open circuit)

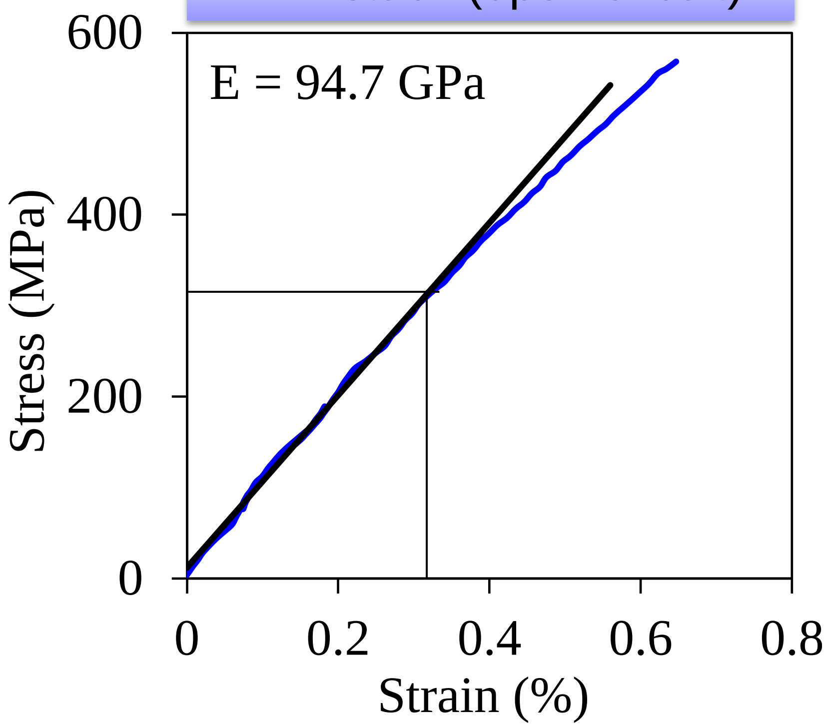


- Stress-strain curves were nonlinearly elastic with failure 0.6% strain
- Nonlinearity was attributed to domain switching mechanism in PZT at higher stresses

S. Yagnamurthy, I. Chasiotis, J. Lambros, R. Polcawich, J. Pulskamp, M. Dubey, “Mechanical and Ferroelectric Behavior of PZT Thin Films,” Journal of Microelectromechanical Systems 20, pp. 1250-1258, (2011).

# PZT Properties in Open and Short Circuit Conditions

PZT curves (extracted from laminas)

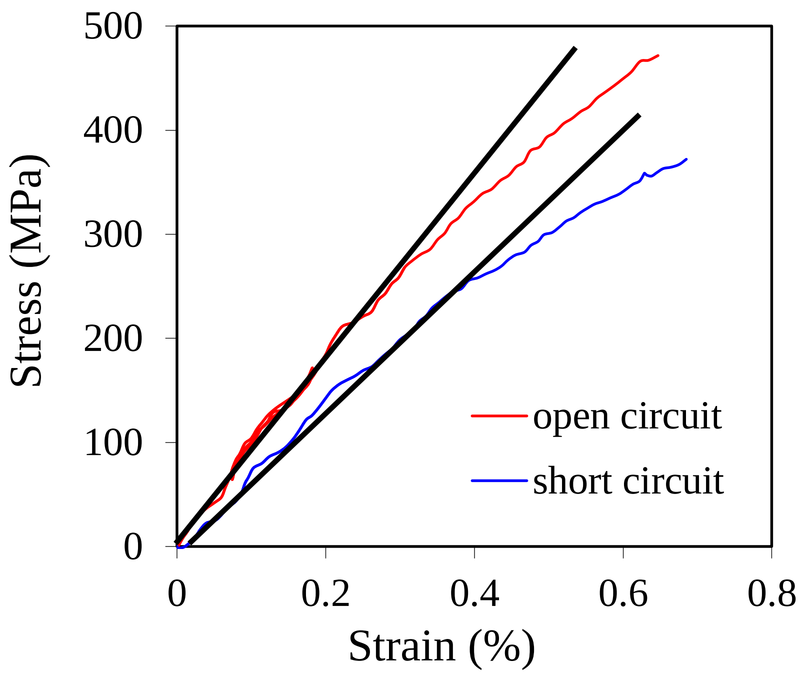


| Material | Modulus (GPa) | $\sigma_{failure}$ (MPa) |
|---|---|---|
| $SiO_2$ | 72.3±2 | 1,170±200 |
| $SiO_2$-Pt | 87.9±1 | 780±70 |
| Pt ** | 182±8 | 1,876±10 |
| $SiO_2$-Pt-PZT | 87.9±1 | 412±50 |
| $SiO_2$-Pt-PZT-Pt | 93.5±2.3 | 511±50 |
| PZT (open circuit) | **84±3** | 510±35 |
| PZT (short circuit) | **60.5±5** | 356±55 |

The modulus of PZT was extracted using simple laminate theory as 84±3 GPa and 60.5±5 GPa for open and short circuit conditions, respectively.


S. Yagnamurthy, I. Chasiotis, J. Lambros, R. Polcawich, J. Pulskamp, M. Dubey, "Mechanical and Ferroelectric Behavior of PZT Thin Films," Journal of Microelectromechanical Systems 20, pp. 1250-1258, (2011).

# Ferroelectric Behavior at High Electric Fields (Low Voltage)

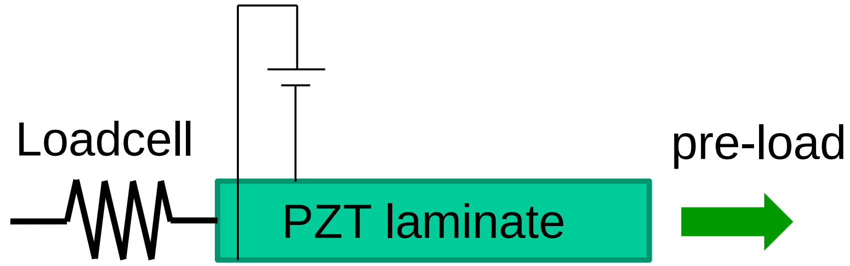


±10 V DC

- Electric field induced stress hysteresis loops were measured with applied pre-stress in the range of 0-600 MPa
- At high applied electric fields (> 2MV m$^{-1}$), the ferroelectric behavior of PZT is due to electrostriction and domain switching
- The electroactive coefficient, $e_{31,eff}$ was used to quantify the ferroelectric behavior of PZT as the ratio of stress to applied electric field:

$$P = e_{31,eff} \cdot \frac{V}{t_{PZT}} \cdot A_{PZT}$$

# Effect of Applied Pre-Stress on Hysteresis Loops

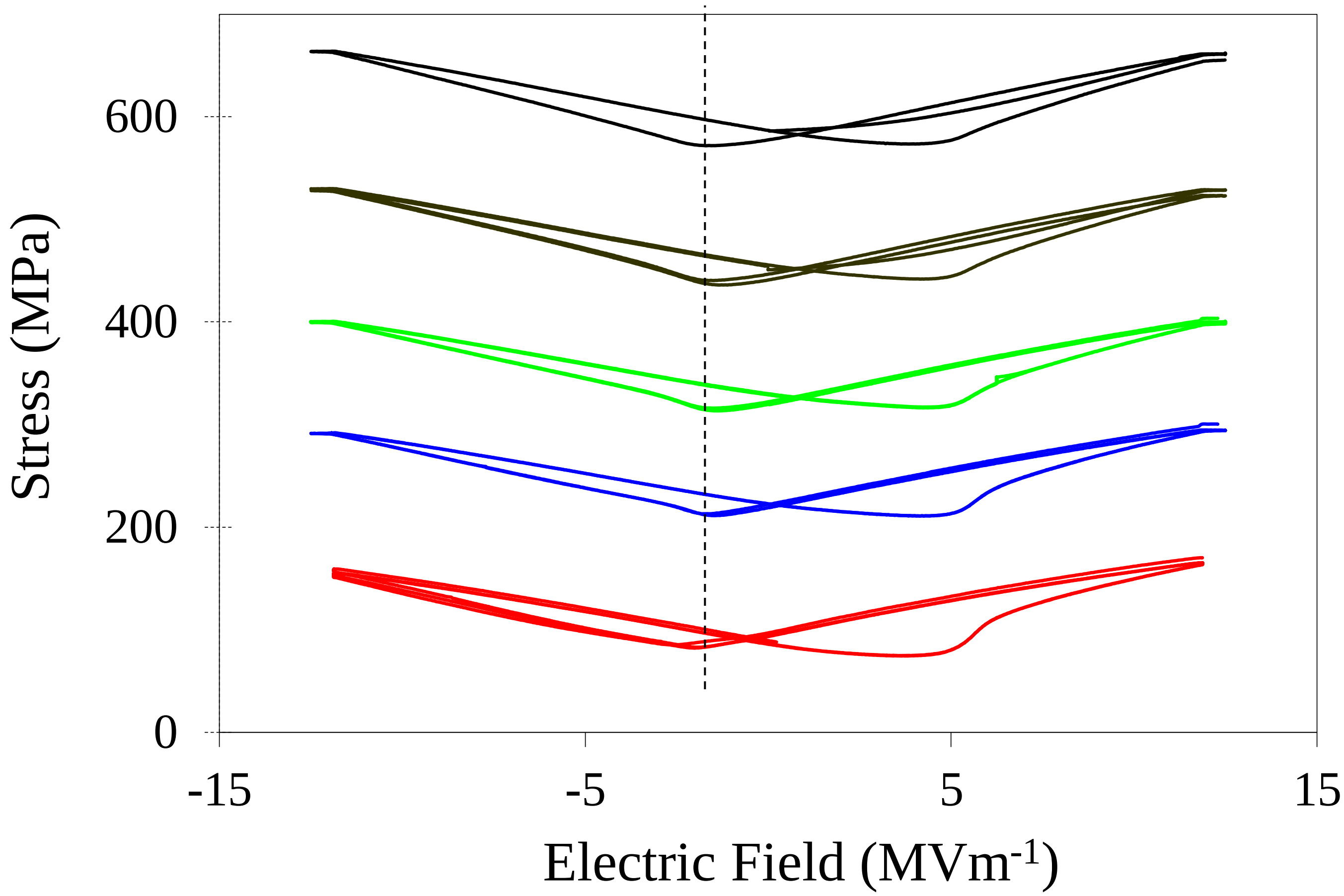


- Stress induced hysteresis loops became symmetric at high applied stresses
- The intersection of the hysteresis loops shifted to positive electric fields.

S. Yagnamurthy, I. Chasiotis, J. Lambros, R. Polcawich, J. Pulskamp, M. Dubey, "Mechanical and Ferroelectric Behavior of PZT Thin Films," Journal of Microelectromechanical Systems 20, pp. 1250-1258, (2011).

# Dependence of Electroactive Coefficient on Pre-stress

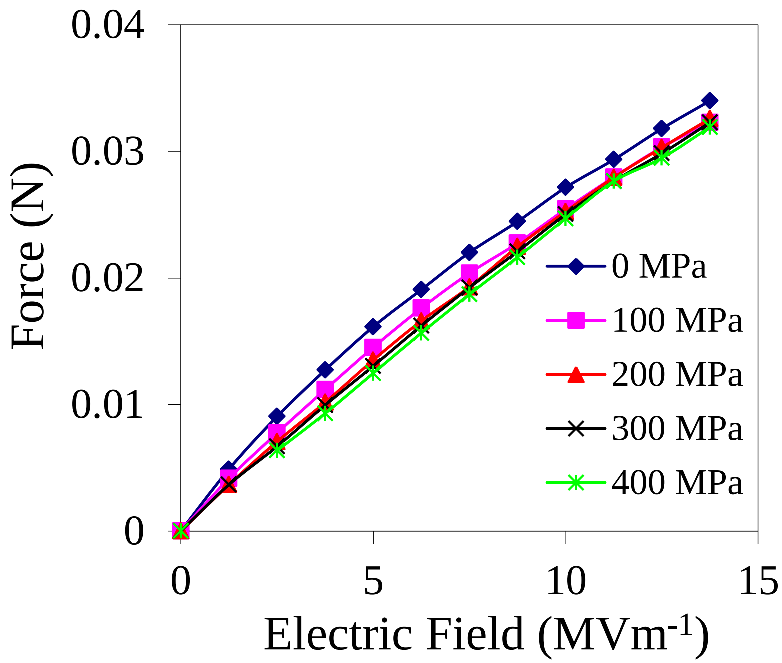


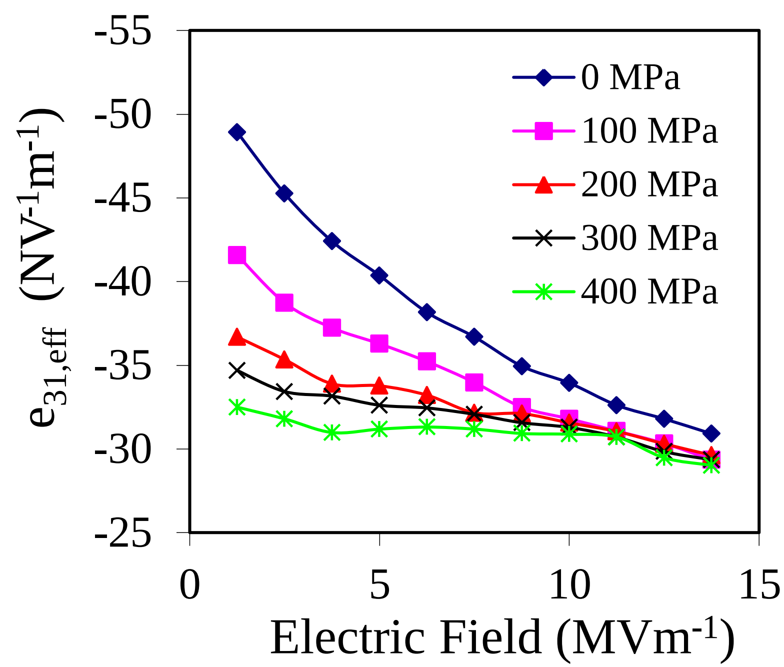


- With no pre-stress, $e_{31,eff}$ varied nonlinearly with applied electric field between -50 $NV^{-1}m^{-1}$ and -30 $NV^{-1}m^{-1}$ and was independent of the applied field at high pre-stress amplitudes.
- Pre-stress lowers domain switching activity in PZT and produces more linear actuation force with the applied electric field.

S. Yagnamurthy, I. Chasiotis, J. Lambros, R. Polcawich, J. Pulskamp, M. Dubey, “Mechanical and Ferroelectric Behavior of PZT Thin Films,” Journal of Microelectromechanical Systems 20, pp. 1250-1258, (2011).

# Conclusions

- Evaluated the effective mode I critical stress intensity factor for laminated and columnar grain polysilicon films as a function of dopant concentration to assess the role of grain heterogeneity and local toughness on crack initiation and arrest
- Quantified the effect of specimen size on fracture strength of polysilicon films via a Weibull analysis to identify the location of failure initiation
- Failure originates in patterning processes rather than deposition: Investigating the effect of removal of sidewall flaws on strength improvement
- Investigating the role of doping using bi-crystal experiments using chevron specimens
- Obtained the electroactive coefficients PZT thin films for MEMS and mechanical properties under open and short circuit conditions: They were the first data of their kind and have drawn interest by industry too.